OPEN

A novel mechanism of protein thermostability: a unique N-terminal domain confers heat resistance to Fe/Mn-SODs

Wei Wang[1,3]*, Ting Ma[1,4]*, Baoliang Zhang[1], Nana Yao[1], Mingchang Li[1], Lianlei Cui[1], Guoqiang Li[1,4], Zhenping Ma[2] & Jiansong Cheng[2]

[1]Key Laboratory of Molecular Microbiology and Technology, Ministry of Education, TEDA Institute of Biological Sciences and Biotechnology, Nankai University, 23 Hongda Street, TEDA, Tianjin 300457, PR China, [2]State Key Laboratory of Medicinal Chemical Biology and College of Pharmacy, Nankai University, Tianjin 300071, PR China, [3]Tianjin Key Laboratory of Microbial Functional Genomics, TEDA, Tianjin 300457, PR China, [4]College of Life Sciences, Nankai University, Tianjin 300071, PR China.

Superoxide dismutases (SODs), especially thermostable SODs, are widely applied in medical treatments, cosmetics, food, agriculture, and other industries given their excellent antioxidant properties. A novel thermostable cambialistic SOD from *Geobacillus thermodenitrificans* NG80-2 exhibits maximum activity at 70°C and high thermostability over a broad range of temperatures (20–80°C). Unlike other reported SODs, this enzyme contains an extra repeat-containing N-terminal domain (NTD) of 244 residues adjacent to the conserved functional SODA domain. Deletion of the NTD dramatically decreased its optimum active temperature (OAT) to 30°C and also impaired its thermostability. Conversely, appending the NTD to a mesophilic counterpart from *Bacillus subtilis* led to a moderately thermophilic enzyme (OAT changed from 30 to 55°C) with improved heat resistance. Temperature-dependant circular dichroism analysis revealed the enhanced conformational stability of SODs fused with this NTD. Furthermore, the NTD also contributes to the stress resistance of host proteins without altering their metal ion specificity or oligomerisation form except for a slight effect on their pH profile. We therefore demonstrate that the NTD confers outstanding thermostability to the host protein. To our knowledge, this is the first discovery of a peptide capable of remarkably improving protein thermostability and provides a novel strategy for bioengineering thermostable SODs.

S uperoxide dismutases (SODs, EC 1.15.1.1) are metalloenzymes that are widely expressed in prokaryotic and eukaryotic cells. SODs catalyse the conversion of superoxide radicals ($O_2{}^{\cdot-}$) to H_2O_2 and O_2, and play a crucial role in the primary cellular defence system against oxidative stress[1]. Four types of SODs have been reported according to their metal cofactors: manganese SOD (Mn-SOD), iron SOD (Fe-SOD), copper/zinc SOD (Cu/Zn-SOD), and nickel SOD (Ni-SOD)[2–4]. Of these, Mn-SOD and Fe-SOD are closely related as their protein structures differ from the other two groups and were recently assigned into one family[5]. Mn-SOD and Fe-SOD are prevalent in bacteria, mitochondria and chloroplasts, and likely evolved from a common ancestor[3,5]. Mn-SOD and Fe-SOD are typically homodimers or homotetramers and generally require either Mn^{2+} or Fe^{2+} to perform their biological activities; however, some SODs, referred to as cambialistic SODs, can accommodate both ions and are often found in anaerobic organisms[5,6].

Over the past 40 years, SODs have attracted tremendous attention and are widely used in the pharmaceutical, cosmetic, food, agriculture, and environmental protection industries due to their excellent antioxidant properties[7–12]. At one time, SODs were isolated from animal or plant sources, but the focus has recently shifted to microbial sources since these organisms can be easily induced and cultivated on a large scale[3]. For industrial applications, thermostability is a major requirement for commercial SODs, because thermal denaturation is a common cause of enzyme inactivation. Fortunately, the isolation of thermostable SODs from thermotolerant or thermophilic microorganisms offers a rapid and effective means to address this issue. To date, many thermostable SODs have been identified from thermophiles and hyperthermophiles, such as *Aquifex pyrophilus*[13], *Sulfolobus solfataricus*[14], *Aeropyrum pernix*[15], *Pyrobaculum aerophilum*[16], *Bacillus stearothermophilus*[17], *Chloroflexus aur-*

antiacus[18], *Thermomyces lanuginosus*[19], *Bacillus licheniformis*[20], *Chaetomium thermophilum*[21], and *Thermus thermophilus*[22]. Recent efforts to improve the thermal resistance of SODs through chemical modification, gene recombination, and simulated SOD compounds have achieved considerable success[23,24]. Bioinformatic methods have also been used to guide the bioengineering process[25]. Nevertheless, the generality of these methods is limited because the determinants of protein thermostability are numerous. Previous studies indicated that SOD thermostability was affected by many factors, such as ion pairs, hydrogen bonds, hydrophobicity, polar interactions, molecular weight and secondary structures[25–29]. Optimising the thermostability of a SOD using more than one strategy could offer significant progress but also faces great challenges[29].

Geobacillus thermodenitrificans NG80-2 is a crude oil-degrading thermophilic facultative anaerobe isolated from a deep-subsurface oil reservoir in Northern China and grows at 45 to 73°C (optimum 65°C)[30]. Analysis of the NG80-2 genome sequence revealed the presence of three putative *sod* genes, *Fe/Mn-sod* (*GTNG_2215*, referred as *sod*$_{NG2215}$ in this study), *Mn-sod* (*GTNG_2400*), and *Cu/Zn-sod* (*GTNG_2884*), which are also present in other species of the *Geobacillus* genus[31]. Of these three genes, *sod*$_{NG2215}$ encodes an unusual SOD comprised of 449 amino acids and is considerably larger than other identified SODs. Apart from the conserved functional SODA domain that belongs to the Fe/Mn-SOD family, SOD$_{NG2215}$ contains an extra 244-amino-acid N-terminal domain (NTD), distinguishing it from the homologous enzymes from other mesophilic species of the *Bacillus* genus. Interestingly, this type of NTD is present in all SOD$_{NG2215}$-like SODs from in *Geobacillus* and contains one or two repeating segments. In this study, the role of the NTD in the activity, structure, thermal resistance, and stress resistance of the host protein was investigated in a detailed manner. The work presented here reveals a special and novel mechanism for protein thermostability and provides a feasible new method to engineer heat-resistant SODs.

Methods

Materials and reagents. The primers were synthesised by the AuGCT Biotechnology Corporation (Beijing, China). Taq DNA Polymerase, dNTP, and restriction enzymes were purchased from TaKaRa (Dalian China). T4 DNA ligase was obtained from Promega (Mannheim, Germany), and the DNase I was procured from Roche (Basel, Switzerland). The Chelating Sepharose Fast Flow column and High Molecular Weight Standards were purchased from Amersham Biosciences (Hammersmith, UK). Phenylmethane-sulfonyl fluoride (PMSF) was purchased from Sigma (St. Louis, Mo, USA). All other chemicals and reagents were from Shanghai Sangon, China.

Bacterial strains and culture conditions. *G. thermodenitrificans* NG80-2 (CGMCC 1228) was grown in Luria-Bertani (LB) medium at 60°C with shaking. *Bacillus subtilis* BSn5 and *Escherichia coli* BL21 (DE3) (Novagen) were grown in LB medium at 37°C with shaking. When necessary, 50 mg kanamycin/L was added to the medium.

Bioinformatics methods. The alignment of SODs from *G. thermodenitrificans* NG80-2 (YP_001126309), *B. subtilis* BSn5 (ADV92836), and their closely related homologs was performed using the ClustalW program[32]. Phylogenetic trees were constructed using the neighbour-joining (NJ) method. Bootstrap values (expressed as percentages of 500 replications) greater than 50% are indicated above the branches. Sequence logos were generated with Weblogo[33].

Cloning and plasmid construction. Genomic DNA from NG80-2 and BSn5 was extracted as described previously[30]. The primers used in this study are listed in Supplementary Table S1. The PCR was initiated by denaturation at 94°C for 3 min followed by 30 cycles of 94°C for 30 s, 55°C for 45 s and 72°C for 2 min and a final extension at 72°C for 5 min. *Sod*$_r$ was amplified using PCR with *sod_N-GTNG_2215* and *sod_C-BSn5* as the templates. The PCR product was digested with *Nde*I/*Hind*III (for *sod*$_{NG2215}$ and *sodA*$_{NG2215}$), *Nde*I/*Bam*HI (for *sodA*$_{BSn5}$ and *sod*$_r$), or *Eco*RI/*Xho*I (for *sod*$_{BSn5}$), and the resulting fragment was ligated into pET-28a (Novagen) to generate the recombinant plasmid. The presence of the insert in the recombinant plasmid was confirmed by sequencing using an ABI 3730 automated DNA sequencer (ABI, Foster City, USA).

Protein expression and purification. *E. coli* BL21 carrying the recombinant plasmid was grown in LB medium containing 50 mg/L kanamycin to an A_{600} nm of 0.6. Protein expression was induced for 3 h using 0.1 mM IPTG at 37°C (for SOD$_{NG2215}$

and SODA$_{NG2215}$), 0.05 mM IPTG at 25°C (for SOD$_{BSn5}$ and SODA$_{BSn5}$), and 0.1 mM IPTG at 30°C (for SOD$_r$).

All steps in the following procedures were performed at 4°C. *E. coli* cells were harvested with centrifugation at 10,000 × *g* for 10 min, washed with lysis buffer (50 mM Tris-HCl, pH 8.0; 300 mM NaCl; 10 mM imidazole), resuspended in the same buffer containing PMSF (1 mM) and lysozyme (1 g/L), and sonicated (Hielscher UP200s ultrasonic processor, 20 kHz, 0.5 cycle, 90% amplitude). After the addition of RNase A (10 μg/mL) and DNase I (5 μg/mL), the lysate was incubated on ice for 15 min, and the crude extract was obtained using centrifugation at 18,000 × *g* for 30 min. The crude extract was applied to a Chelating Sepharose Fast Flow column according to the manufacturer's instructions. Unbound proteins were removed with wash buffer (50 mM Tris-HCl, pH 8.0; 300 mM NaCl; 20 mM imidazole). His-tagged recombinant proteins were eluted with elution buffer (50 mM Tris-HCl, pH 8.0; 300 mM NaCl; 250 mM imidazole) and dialysed against 50 mM Tris-HCl (pH 8.0) containing 20% glycerol.

The protein concentration was determined using the Bradford method[34]. Sodium dodecyl sulphate polyacrylamide gel electrophoresis (SDS-PAGE) was performed according to the method described by Laemmli[35].

SOD activity assay. SOD activity was measured using the method of Beauchamp and Fridovich[36]. Briefly, the 3-ml reaction mixture contained 13 mM L-methionine, 63 μM nitroblue tetrazolium (NBT), 1.3 μM riboflavin, 10 μM EDTA-Na$_2$, and 10 μL purified enzyme in 50 mM potassium phosphate buffer (pH 7.8). The test tubes were exposed to a source of light. The reduction of NBT was monitored after 10 min at 560 nm. One unit of SOD activity was defined as the amount of enzyme that caused 50% of maximum inhibition of the NBT reduction. All assays were performed in triplicate, and average values were reported. Activity was estimated as a percentage of the maximum.

Metal reconstitution and analysis. The apoprotein was prepared from purified SOD using dialysis against a solution of 20 mM 8-hydroxyquinoline, 2.5 mM guanidium chloride, 50 mM Tris and 0.1 mM EDTA at pH 3.8 for 24 h at 4°C. The SOD apoprotein was then reconstituted through dialysis with 50 mM Tris buffer (pH 7.8) containing 1 mM ferrous ammonium sulphate or 1 mM manganese chloride for 18 h at room temperature. Then, the solution was subject to further dialysis against the same buffer to remove excess amounts of metal salts[37].

Metal analysis and quantification were performed using a 180-80 Polarized Zeeman atomic absorption spectrophotometer. A manganese standard curve was obtained using 0.1% nitric acid and Mn^{2+} concentrations of 1.0, 2.0, and 4.0 μg/L. Similarly, an iron standard curve was obtained using 0.1% nitric acid and Fe^{2+} concentrations of 1.0, 2.0, and 4.0 μg/L. The absorbencies of manganese and iron were measured at 297.5 and 248.3 nm, respectively. The SOD samples were diluted in nanopure water with 0.1% nitric acid until the absorbance was within the range of the standard curves. The samples were thoroughly dialysed in 20 mM Tris (pH 8.0) prior to the assay.

Effects of temperature and pH on SOD activity. To determine the optimum temperature, SOD activity was measured in the standard reaction mixture at pH 7.8 at temperatures ranging from 20 to 80°C. To determine the optimum pH, SOD activity was measured at the optimum temperature in the pH range of 3.0 to 10.0 using sodium citrate (pH 3.0–8.0), Tris-HCl (pH 8.0 and 9.0), or glycine-NaOH (pH 9.0 and 10.0) buffers. Activity was measured as a percentage of the maximum.

Thermostability test. The thermal stability of SOD was tested after incubating samples at 20, 30, 40, 50, 60, 70, and 80°C for 10, 20, 30, 40, 50 and 60 min without substrate. The remaining activities of enzymes were detected at their optimum temperature and pH and calculated as the percentage of the maximum SOD activity.

Analytical ultracentrifugation. Sedimentation velocity experiments were performed in a ProteomeLab XL-1 Protein Characterization System (Beckman Coulter). All interference data were collected at a speed of 42,000 rpm in an An-60 Ti rotor at 4°C. A set of 200 scans was collected at 6-min intervals. The proteins were prepared in 50 mM potassium phosphate buffer plus 150 mM NaCl at pH 6.8 for SOD$_{NG2215}$, SODA$_{NG2215}$, and SOD$_r$ and at pH 7.8 for SOD$_{BSn5}$ and SODA$_{BSn5}$. The data were analysed using the program SEDFIT (version 11.8) in terms of a continuous c(s) distribution.

Effects of inhibitors, detergents, and denaturants on SOD activity. The effects of inhibitors (ethylenediaminetetraacetic acid (EDTA) and β-mercaptoethanol (β-ME)), detergents (sodium dodecyl sulphate (SDS)), and denaturants (urea and guanidine guanidine hydrochloride) on SOD activity were investigated according to the method described by Zhu[38].

Circular dichroism (CD). Circular dichroism was measured on a Jasco J-715 circular dichroism spectrometer (Japan). First, 0.14 mg/mL SOD$_{BSn5}$ and 0.4 mg/mL other proteins including SOD$_{NG2215}$, SODA$_{NG2215}$ SODA$_{BSn5}$ and SOD$_r$ in 20 mM potassium phosphate buffer (pH 8.0) was placed in a 1 mm quartz cell. All spectra were recorded at a scanning rate of 100 nm/min with 0.1 nm wavelength steps from 190 to 250 nm and three accumulations.

Structural modelling. The structure of SODA$_{NG2215}$, the functional domain of SOD$_{NG2215}$, was modelled via the SWISS-MODEL server (http://swissmodel.expasy.org/).

The structure of a closely related iron SOD from the strain *M. thermautotrophicus* Delta H, which has a 52% sequence identity and 67% sequence similarity with SODA$_{NG2215}$, was used as a template. The stereochemical and overall quality of the final model was assessed using PROCHECK and ProSA. In the resulting model, 89% of the residues were in the most favoured regions, and no residues were located in disallowed regions. The PROCHECK overall g factor evaluating all torsion angles and bond lengths was 0.08, indicating a high-quality model. The ProSA Z score of the SODA$_{NG2215}$ model was calculated as −6.03. Z scores for experimentally determined X-ray structures of proteins with a similar size (around 207 amino acids) lie in the range of −1 to −10.8. The Z score of this model was thus within the range of scores typical for similarly sized native proteins.

Results

Bioinformatic analysis of SOD$_{NG2215}$. SOD$_{NG2215}$ possesses a unique repeat-containing N-terminal domain (NTD) that differs from its closely related homologues from *Bacillus*. The functional domains (SODA) of SOD$_{NG2215}$-like SODs from *Geobacillus* are conserved (preliminary sequence identity: 84–93%) and are also highly similar to their counterparts from *Bacillus* (preliminary sequence identity: 64–71%). Alignment of the SOD$_{NG2215}$-like SODs from 13 thermophilic *Geobacillus* strains showed that these SODs have an extra N-terminal segment despite their various lengths (Supplementary Fig. S1). A blast analysis revealed that these segments share significant amino acid similarity with each other but not with other sequences in GenBank. Further alignment of these N-terminal segments revealed that the eight SODs (subgroup 1) harbour two repeat sequences within their extra N-terminal segments, whereas the other four (subgroup 2) only have a single repeat sequence (Fig. 1b, c). Due to the presence of these extra segments in SOD$_{NG2215}$-like SODs from all thermophilic *Geobacillus* but not in SODs from any *Bacillus* species, these repeat-containing domains were thus proposed to be involved in the thermostability maintenance of SODs. However, whether the repeat sequence forms a special secondary structure remains unknown. The phylogenetic trees of both the N- and C-terminal domains of *Geobacillus* SODs exhibited highly similar topological structures (Fig. 1a,b), indicating that the *sod* genes potentially gained their extra NTDs before the divergence at nodes N1 and N2 occurred.

Gene manipulation, expression, and purification of SOD variants. To explore the role of the SOD$_{NG2215}$ NTD, we constructed five recombinant clones (Fig. 2a) to comparatively study the thermostability, temperature-induced conformational changes, and stress resistance of the corresponding recombinant proteins. First, the full-length *sod*$_{NG2215}$ and the NTD-deleted form (*sodA*$_{NG2215}$) were separately cloned to study the effects of the NTD in its natural host. To further investigate its effects on other Fe/Mn SODs, the NTD was fused to a Fe/Mn SOD from a mesophilic strain of *B. subtilis* BSn5 (SOD$_{BSn5}$), which shares 66% amino acid sequence identity with SOD$_{NG2215}$. The resulting construct (*sod*$_r$) contained the DNA segments encoding the SOD$_{NG2215}$ NTD and the SODA domain of SOD$_{BSn5}$. The SODs from *Bacillus* are the closest phylogenetically to the SODs from *Geobacillus* (Fig. 1a) and typically exhibit poor heat-resistance[39]. The full-length *sod*$_{BSn5}$ and *sodA*$_{BSn5}$ genes encoding the C-terminal SODA domain were also cloned as negative controls.

SDS-PAGE analysis showed that all five SOD proteins were expressed accordingly to their expected sizes (Fig. 2b).

Removing the NTD does not alter the metal ion specificity of the host SOD. To investigate the metal ion preference of SOD$_{NG2215}$ and its NTD-deleted form, SODA$_{NG2215}$ Fe^{2+}- and Mn^{2+}-reconstituted enzymes were prepared. As shown in Supplementary Table S2, an atomic absorption analysis demonstrated that each monomer of the
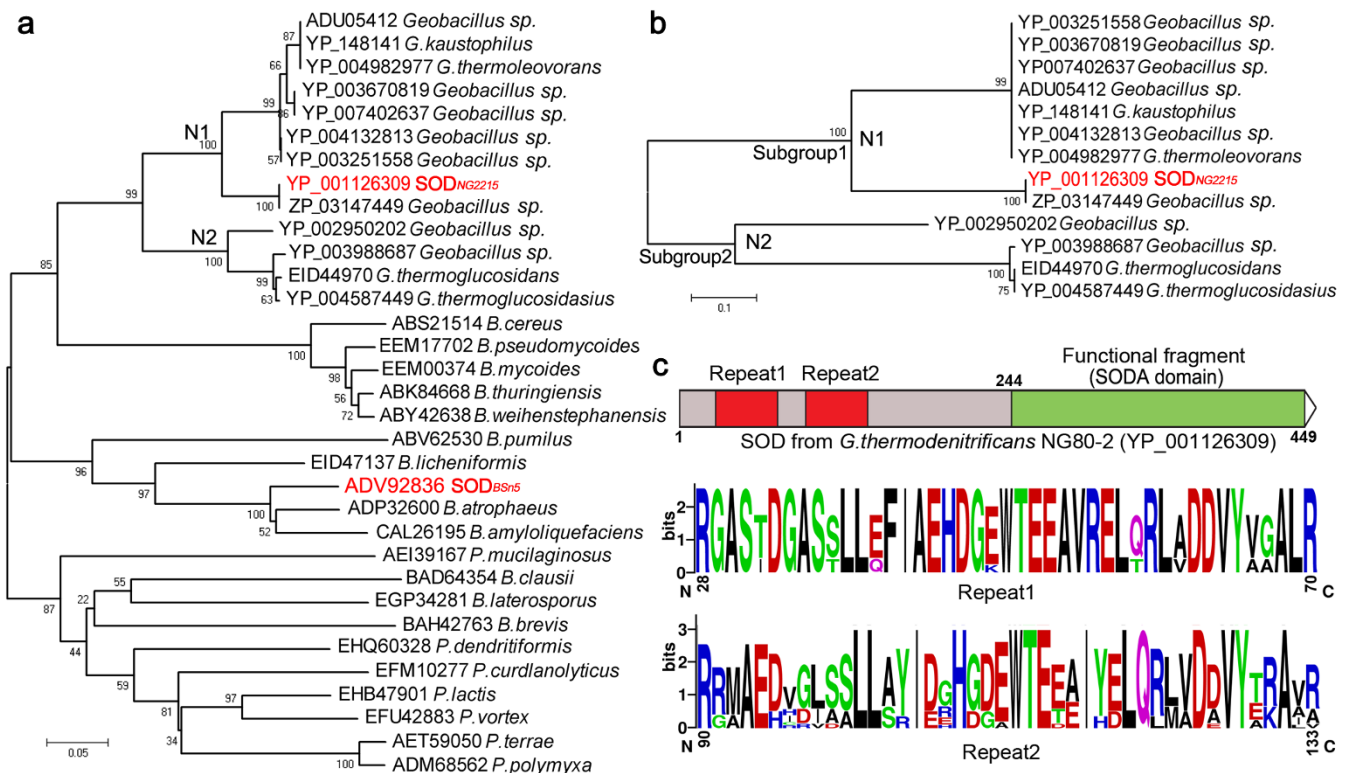

Figure 1 | Phylogenetic analysis of C-terminal (functional) fragments (a) and N-terminal fragments (b) of SODs from *G. thermodenitrificans* NG80-2 (YP_001126309), *B. subtilis* BSn5 (ADV92836), and their closely related homologs. The accession number of each SOD in GenBank is labelled prior to the species name. The proteins used for the activity test in this study are highlighted in red. The sequence logos of the repeat sequences were constructed from alignments of SOD N-terminal fragments from the 13 *Geobacillus* strains (c). The letter size is proportional to the degree of amino acid conservation. The deletion (gap) is represented by the letter "B".
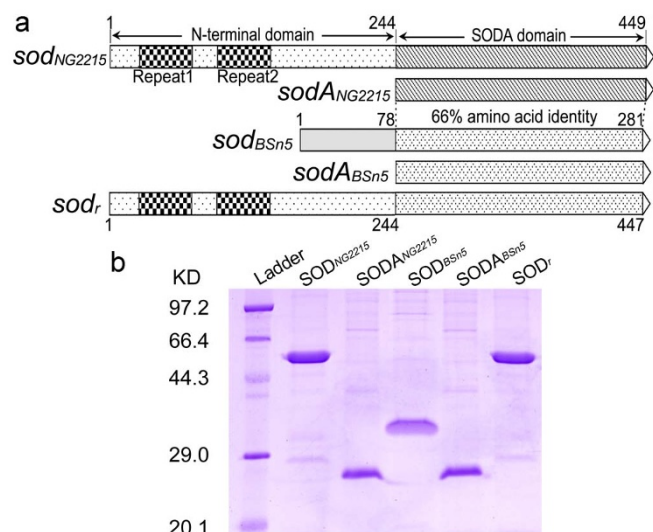
Figure 2 | A schematic illustration of the various constructs (a) and the SDS-PAGE analysis of the purified SOD proteins (b). Proteins were stained with Coomassie brilliant blue. Ladder, standard protein size marker. The expected sizes of SOD_{NG2215}, $SODA_{NG2215}$, SOD_{BSn5}, $SODA_{BSn5}$, and SOD_r were 54.0 kD, 26.6 kD, 37.3 kD, 26.3 kD, and 53.6 kD, respectively.

native SOD_{NG2215} was associated with 0.55 ± 0.03 atoms of iron and 0.10 ± 0.01 atoms of manganese, whereas 0.73 ± 0.02 atoms of iron and 0.81 ± 0.03 atoms of manganese were associated with the Fe^{2+}- and Mn^{2+}-reconstituted SOD_{NG2215} enzymes per subunit, respectively. The Fe^{2+}- and Mn^{2+}- reconstituted SOD_{NG2215} exhibited specific activities of 769.1 ± 17.2 and 1158.4 ± 29.3 U/mg, respectively; the apoprotein was inactive. The Mn^{2+}-reconstituted SOD_{NG2215} was approximately 40 to 50% more active than the native and Fe^{2+}-reconstituted SOD_{NG2215}, suggesting that SOD_{NG2215} is a cambialistic SOD that can accommodate both Fe^{2+} and Mn^{2+} as cofactors with manganese preferred over iron in regard to enzymatic activity. The metal ion specificity study of $SODA_{NG2215}$ revealed similar characteristics only with less enzymatic activity than SOD_{NG2215} (Supplementary Table S2). This result indicates that the NTD has no effect on the metal ion specificity of SOD.

Oligomerisation form and composition of SOD are not altered by the NTD. Analytical ultracentrifugation analysis (Fig. 3) indicates that either the full length SOD_{NG2215} or the NTD-deleted form of $SODA_{NG2215}$ exist mainly in a tetrameric form. SOD_{Bsn5} and its counterparts, $SODA_{Bsn5}$ and NTD-fused SOD_r, were found in dimeric and monomeric forms with no tetramer detected. The extremely increased peak area ratio of the tetramer compared with the monomer indicates most protein molecules of SOD_{NG2215} and $SODA_{NG2215}$ tend to form multimers, whereas all three SOD_{Bsn5}-derived proteins prefer to exist in monomeric forms. It thus seems that the functional SODA domain of the SOD variants determines the formation of oligomerisation, whereas the NTD has no effect on the oligomerisation form or the monomer-multimer ratio.

NTD contributes to host thermophilicity with a slight alteration in pH profiles. The optimum active temperature (OAT) was determined by testing the SOD activity at temperatures ranging from 20 to 80°C (Fig. 4a). The OAT for SOD_{NG2215} was 70°C, which is close to that of other thermophile-derived SODs (50–70°C)[17,40] but lower than that of the hyperthermophilic SODs (87–95°C)[14,16]. $SODA_{NG2215}$, SOD_{BSn5}, and $SODA_{BSn5}$ exhibited mesophilic properties with OATs of 30°C, 35°C and 30°C, respectively. Intriguingly, SOD_r exhibited optimal activity at 55°C, and retained 46% of its maximum activity even at 80°C. Clearly, the NTD-fused proteins of SOD_{NG2215} and SOD_r
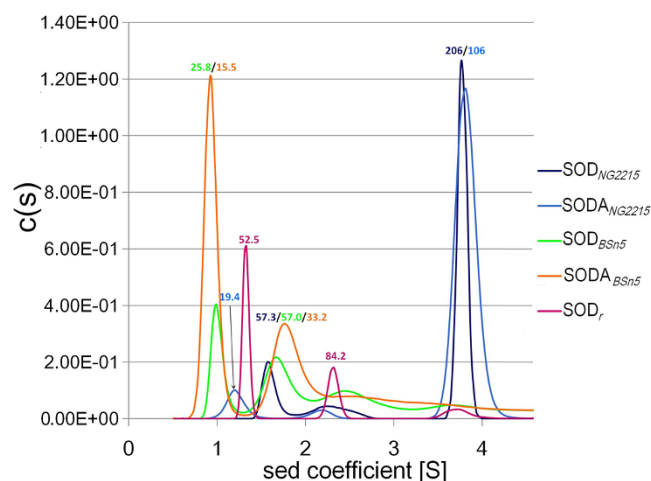

Figure 3 | Analysis of the oligomerised forms of five SOD proteins. The size of SOD_{NG2215}, $SODA_{NG2215}$, SOD_{BSn5}, $SODA_{BSn5}$ and SOD_r (all at 0.05 mM) were determined using analytical ultracentrifugation. The estimated molecular masses (kDa) are provided above the peaks.

are considerably more thermophilic than their counterparts without the NTD ($SODA_{NG2215}$, SOD_{BSn5}, and $SODA_{BSn5}$).

Although the relative activities were used for the comparison of the thermophilicities of the variant SODs, the real activities of these recombinants are quite different. The initial enzymatic activities of SOD_{NG2215}, $SODA_{NG2215}$, SOD_{BSn5}, $SODA_{BSn5}$ and SOD_r investigated at 20°C are 800.9 ± 18.3, 837.1 ± 19.2, 682.3 ± 14.6, 598.8 ± 16.2 and 678.3 ± 15.1 U/mg, respectively, whereas the maximum at their individual OATs rise to 1132.2 ± 20.6 (70°C), 915.9 ± 18.9 (30°C), 933.0 ± 19.1 (35°C), 752.5 ± 17.5 (30°C), and 1055.1 ± 20.3 (55°C) U/mg, respectively.

The pH profiles of the SOD activity are presented in Figure 4b. SOD_{NG2215} and $SODA_{NG2215}$ exhibited maximum activities at pH 4 and 5–6, respectively, indicating that they are both acidophilic. Outside their optimum pH ranges, the activities of both enzymes quickly decreased. To our knowledge, SOD_{NG2215} is the most acidophilic, thermophilic, cambialistic SOD that has been reported to date. In contrast, SOD_{BSn5}, $SODA_{BSn5}$ and the NTD fused SOD_r were all neutrophilic with an optimum pH of around 8. Therefore, the NTD showed negligible effects on the pH preference of SOD activities.

NTD plays an important role in maintaining the thermostability of SODs. An optimum active temperature assay demonstrated that the presence of the NTD alters the thermophilicity of SODs. Therefore, we further examined the role of the NTD in SOD thermostability.

As shown in Figure 5, all enzymes were very stable at a low temperature (20°C) and almost fully active after 60 min. However, the enzymes exhibited variable stability when the temperature was greater than 40°C. $SODA_{NG2215}$, SOD_{BSn5} and $SODA_{BSn5}$, which are mesophilic, also demonstrated poor thermostability when the temperature was greater than 40°C. All three enzymes lost approximately 90% of their activity after 60 min above 60°C and were almost inactive after 10 min at 80°C.

In contrast, the thermophilic SOD_{NG2215} exhibited excellent thermostability over a range of temperatures below 70°C and still remained 70% active after 60 min at 70°C. Even at 80°C, SOD_{NG2215} remained 52% active after 10 min and almost maintained at this level until 60 min. SOD_r, the NTD fused $SODA_{BSn5}$, also exhibited good thermostability (retained 80% and 61% active at 50°C and 60°C, respectively, after 60 min), indicating that this enzyme acted more like a moderate thermophilic Mn-SOD from *B. licheniformis*[20].
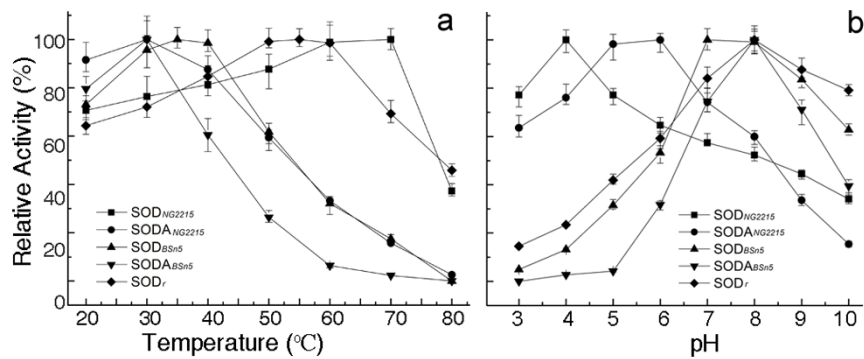
4

Figure 4 | Effects of temperature and pH on SOD activity. The temperature profiles were determined by assaying the activity of purified SOD at temperatures ranging from 20 to 80°C (a). The activity at the optimum temperature was defined as 100%. Each point represents the mean (n = 3) ± standard deviation. The activity of purified SOD was evaluated in buffers ranging from pH 3 to 10 (b). The activity at the optimum pH was defined as 100%. Each point represents the mean (n = 3) ± standard deviation.

Meanwhile, the half-lives and D-values deduced from thermo-stability assays clearly showed that the NTD fused SODs were much more stable than their counterparts without the NTD especially at high temperatures (Supplementary Table S3).

CD spectroscopy analysis reveals the enhanced conformational stability of NTD-fused SODs. Far-UV CD spectra of five SODs exhibited a positive maximum at 192 nm and double-lobed negative peaks at 208 nm and 222 nm, which are characteristic of the high α-helix content of the protein[41,42] (Fig. 6). However, temperature-dependent CD measurements clearly indicated that

the conformational changes of SOD_{NG2215} and SOD_r are quite small compared with the other three counterparts, which is consistent with the results from the temperature-dependent activity assays. The CD signal intensity almost did not decrease further when the temperature rose from 70 to 90°C. Additionally, strikingly reduced ellipticity signals at 192 nm and 208 nm for $SODA_{NG2215}$, SOD_{BSn5}, and $SODA_{BSn5}$ resulted in a sharp isodichroic point at 202 nm, indicating a two-state helix-coil transition[43]. In contrast, the isodichroic points for SOD_{NG2215} and SOD_r are not obvious. When the Spectra was measured at 5°C intervals (Supplementary Fig. S4), an apparent isodichroic point was observed at 201 nm for both SOD_{NG2215} and SOD_r. In addition, the magnitudes at 222 and 208 nm decreased very slightly when the temperature crossed from 70°C to 85°C.

The NTD enhances the host proteins' abilities to resist inhibitors, detergents, and denaturants. The effects of various inhibitors, detergents, and denaturants on SOD activity were examined using EDTA, β-ME, SDS, urea, and guanidine hydrochloride (Fig. 7 and Supplementary Table S4). SODs fused with the NTD are considerably more resistant to these stresses than their counterparts lacking the NTD. Of these stresses, the NTD confers an extraordinary ability to resist denaturants. When tested with urea or guanidine hydrochloride at a final concentration of 2.5 M, 72–93% of the relative activities of SOD_{NG2215} and SOD_r were maintained. In contrast, only 43–64% of their activities remained in their counterparts without the NTD. Additionally, SOD_{NG2215} and SOD_r maintained greater than 45% of their relative activities in SDS at a concentration of 1%, whereas the other SODs were completely repressed.

Figure 5 | Thermostability of purified SOD_{NG2215} (a), $SODA_{NG2215}$ (b), SOD_{BSn5} (c), $SODA_{BSn5}$ (d) and SOD_r (e). The enzyme was pre-incubated at various temperatures (20–80°C, steps of 10°C), and aliquots were withdrawn every 10 minutes to test the residual activities at the optimum temperature and pH by using the standard assay described in the Methods section. The activity of non-heated SOD was defined as 100%. Each point represents the mean (n = 3) ± standard deviation.

Structural modelling and analysis reveal a conserved backbone structure shared by $SODA_{NG2215}$ and its homologs. The structures of several SODs, including those from *M. thermautotrophicus* (1MA1, tetrameric), *A. pernix* (3AK3, tetrameric), *P. aerophilum* (3EVK, tetrameric), *S. acidocaldarius* (1B06, tetrameric), and *S. solfataricus* (1WB8, dimeric), which fall under the same branch as $SODA_{NG2215}$, have been reported.

The structure of $SODA_{NG2215}$, the functional domain of SOD_{NG2215}, modelled based on the structure of a closely related iron SOD from *M. thermautotrophicus* Delta H, which has 52% sequence identity and 67% sequence similarity with $SODA_{NG2215}$. The model of $SODA_{NG2215}$ demonstrated good superimposition with 1MA1, 3AK1, 3EVK, 1B06, and 1WB8 with rmsd values of 0.061, 0.513, 0.501, 0.697, and 0.763, respectively. In addition to the similar back-bone structure, the metal binding residues (Fig. 8) are also conserved among the thermophilic Fe-SODs.
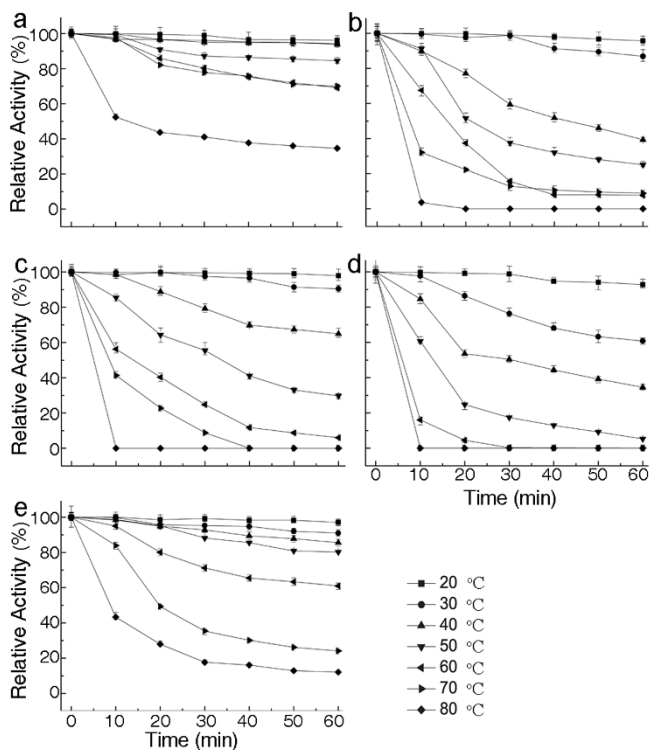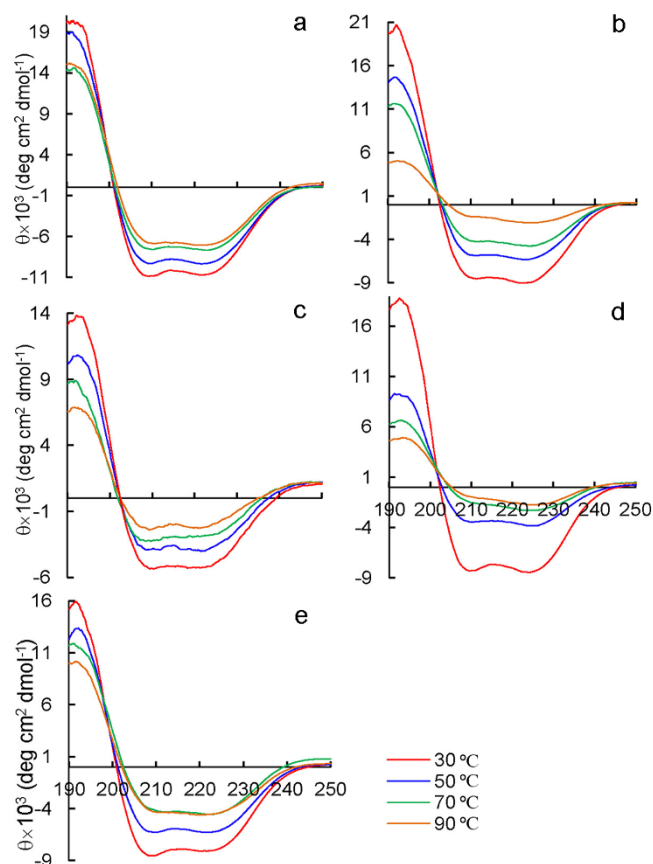
Figure 6 | Temperature-dependent CD spectra of SOD$_{NG2215}$ (a), SODA$_{NG2215}$ (b), SOD$_{BSn5}$ (c), SODA$_{BSn5}$ (d), and SOD$_r$ (e).

Discussion

Three types of SODs (Fe/Mn-SOD, Mn-SOD and Cu/Zn-SOD) are found in thermophilic *Geobacillus*, of which Mn-SOD was identified as being considerably thermostable[38]. In this study, we investigated the thermostability of SOD$_{NG2215}$, a cambialistic SOD from the fac-

ultative anaerobic *G. thermodenitrificans* NG80-2, which can function with both Fe^{2+} and Mn^{2+} as cofactors. Cambialistic SODs can be divided into two groups. One group exhibits approximately equal activity in the Mn^{2+} and Fe^{2+} forms, whereas the other group prefers manganese over iron in regard to enzymatic activity[44]. The former group is often found from anaerobes and the latter is from aerobes or facultative anaerobes[15]. Clearly, SOD$_{NG2215}$ belongs to the latter group.

Geobacillus is a phenotypically and phylogenetically coherent genus of thermophilic bacilli and was recently separated from the genus *Bacillus*[45]. Sequence analysis has revealed that the SOD$_{NG2215}$-like proteins from *Geobacillus* all contain unique NTDs that are not present in other mesophilic *Bacillus* species. The NTDs are thought to be involved in maintaining the thermostability of these SODs (Fig. 1 and Supplementary Fig. S1). Of considerable interest is a 40-amino-acid sequence that is repeated either once or twice within the NTDs and is exclusive to SOD$_{NG2215}$ homologs from *Geobacillus*. The phylogenetic analysis of currently known thermostable Fe-, Mn- or Fe/Mn- SODs from various microorganisms showed that these SODs were roughly split into three major branches except for a Mn-SOD from *Thermoascus aurantiacus* and a Fe-SOD from *Thermosynechococcus elongates*, with that the phylogeny and metal specificity of these thermophilic SODs are not congruent (Supplementary Fig. S2). The Fe/Mn-SOD (SOD$_{NG2215}$) and Mn-SOD (GTNG_2400) from *G. thermodenitrificans* NG80-2 are located in two distinct subgroups. Given their differing protein sizes and ion requirements, it appears that these two SODs may have divergently evolved. SOD$_{NG2215}$ and one of its closely related homologs from *Geobacillus* sp. EPT3, which was previously identified as a Mn-SOD[38], cluster into a same branch with five other SODs derived from different species. However, SOD$_{NG2215}$ and Mn-SOD from EPT3 may adopt completely different thermophilic adaptation strategies compared to five other SODs because the NTD deleted SODA$_{NG2215}$ is more like a mesophilic enzyme. In this study, we provided strong evidence that the NTD containing two repeat sequences contributed to SOD thermostability. Further work to determine the crystal structure and characterise the NTDs containing only a single repeat sequence will help to elucidate the specific role that these sequences play in thermostability.
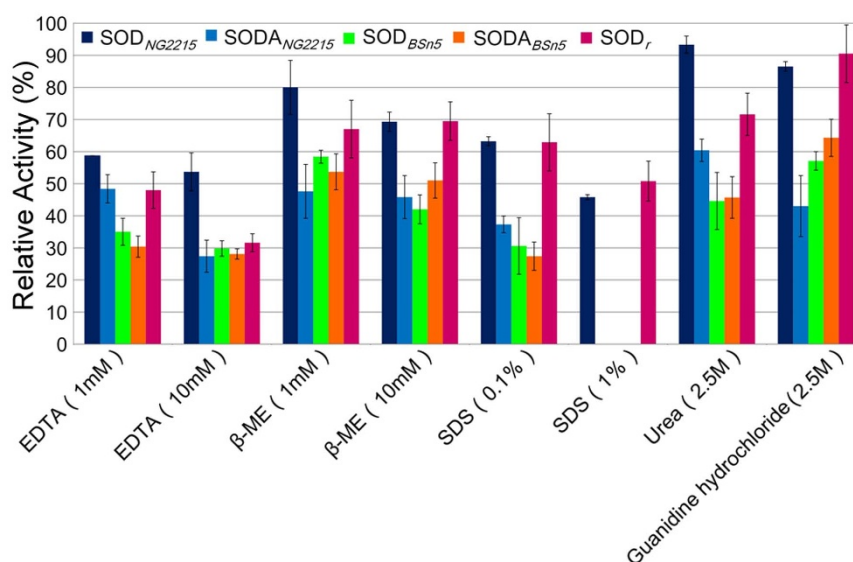

Figure 7 | Effects of inhibitors, detergents, and denaturants on SOD activity. The enzyme was incubated with each inhibitor, detergent, or denaturant at various final concentrations in 50 mM sodium phosphate buffer (pH 7.8) at 25°C for 30 min. Residual activities were measured by the standard assay as described in the Methods section. The reaction mixture without inhibitor, detergent, or denaturant was used as a control and defined as 100%. The values are the mean ± standard deviation from three separate replicates. No enzymatic activities of SODA$_{NG2215}$, SOD$_{BSn5}$ and SODA$_{BSn5}$ were detected with 1% SDS.
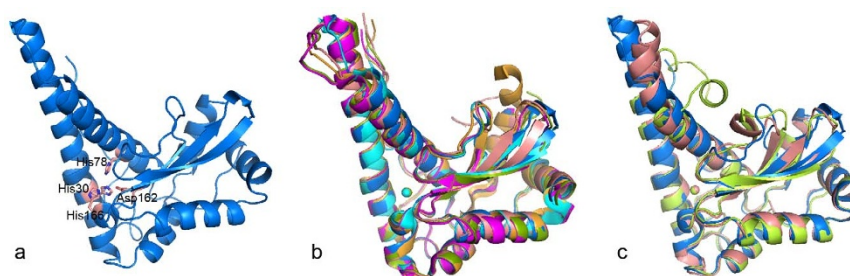
Figure 8 | The model of SODA$_{NG2215}$ generated based on an iron SOD from *M. thermautotrophicus* Delta H (a). Superposition of the SODA$_{NG2215}$ model with 1MA1, 3AK1, 3EVK, 1B06 and 1WB8 (b) as well as structures (1ISA and 1MSD) of SODs from *E. coli* and humans (c).

The finding that the optimum active temperature of the NTD-deleted SODA$_{NG2215}$ decreased dramatically from 70 to 30°C suggests that the NTD plays an essential role in maintaining the high thermo-tolerance of SOD$_{NG2215}$. In contrast, when the NTD was fused with SODA$_{BSn5}$, a mesophilic SOD, the resulting enzyme (SOD$_r$) exhibited remarkably enhanced thermophilicity. The detailed assessment of thermostability also demonstrated that the thermostability of SOD$_r$ is significantly enhanced compared with SOD$_{BSn5}$ and SODA$_{BSn5}$. All these findings indicate that the NTD of SOD$_{NG2215}$ is capable of enhancing the thermophilicity as well as the thermostability of other mesophilic SOD homologs. Futhermore, the comparison of five SOD proteins' Teq values calculated according to the Equilibrium Model (Supplementary Fig. S5 and Table S5) indicated that the NTD also increased the estimated optimum working temperature range[46,47]. It is worth mentioning that although SOD$_{BSn5}$ has a small N-terminal peptide containing 78 residues that is absent in SODA$_{BSn5}$, it only slightly affects the thermophilicity and enzymatic activity.

Some previous studies on cambialistic SODs found that they were more thermostable when reconstituted with manganese rather than iron[15,48]. The thermostability of Mn^{2+}- or Fe^{2+}-reconstituted SOD$_{NG2215}$ and SODA$_{NG2215}$ were also investigated in the present work (Supplementary Fig. S3). The trends chart of the thermostability of both enzymes at 70°C revealed that the Mn^{2+}-reconstituted proteins are considerably more stable than the Fe^{2+}-reconstituted SODs and as stable as the native SODs. Importantly, when the NTD is deleted, the Mn^{2+}-reconstituted SODA$_{NG2215}$ still exhibited poor stability at high temperatures, and its thermostability was even worse than the Fe^{2+}-reconstituted SOD$_{NG2215}$, which contains the NTD. Thus, the effect of the NTD is much more important than the ion constitution in regards to the thermostability of SOD$_{NG2215}$.

Enzymes isolated from thermophilic (50–80°C) or hyperthermophilic (>80°C) microorganisms are generally more thermostable and more resistant to enzyme inhibitors, protein detergents, pH, and other denaturing agents compared with SODs from mesophilic (25–50°C) or psychrophilic (<25°C) microorganisms[49,50]. These enzymes therefore have the potential to be widely used in industrial capacities. Factors contributing towards thermostability of proteins are numerous and complex, such as certain types of amino acids[51], residue contributions to VdW interaction energies[52], increase in hydrophobicity[53,54], differences in compactness[55] and packing density[56], significant changes in hydrogen bonding networks[57], enhancement of secondary structure propensity[58], extensive ion pair interactions[59], differences in the number of amino acids comprising the loops[60], and even a single amino acid mutation far from the active site[24,61]. Therefore, it is extremely difficult to bioengineer a specific enzyme with improved thermostability by using a "universal" method. The discovery that fusion with the NTD from SOD$_{NG2215}$ can significantly improve the thermostability of host SODs provides an easy and feasible method to generate heat-resistant SOD proteins. A similar example has been reported that the N-terminal domain of a multi-functional cellulase EGXA increased the enzyme's thermostability (only tested on 45°C) to a slight extent, while the mechanism

might be different since the N-terminal domain was identified as a cellulose-binding domain and only selectively enhanced enzymatic activity and thermostability towards some of substrates[62]. In addition to thermostability enhancement, the NTD also significantly improved the stress resistance of the host SOD proteins. For all of the tested stresses of inhibitors, detergents, and denaturants in this study, SOD$_{NG2215}$ and the NTD-fused SOD$_r$ both demonstrated enhanced resistance compared with their counterparts without the NTD (Fig. 7 and Supplementary Table S4).

All known thermophilic Fe-SODs except the SOD$_{NG2215}$-like proteins from *Geobacillus* are similar in protein size (20 kD), backbone structure, and metal binding residues (Fig. 8 and Supplementary Fig. S2). Despite such similar features, their thermal stability is remarkably different. It was believed that α-helical content, α-helix length, and even the salt bridges formed by the charged residues, such as Arg and Glu, are important factors for Fe-SOD thermostability. In contrast, the β-strand is negatively correlated via a principal component analysis of five thermophilic SODs and six mesophilic counterparts[25]. Superimposing this model with SOD structures (1MA1, 3AK1, 3EVK, 1B06, and 1WB8) revealed that these tertiary structures are well conserved, especially the regions around the ion binding site. Evidence from metal reconstitution analysis and density gradient centrifugation indicated that the NTD of SOD$_{NG2215}$ did not affect the metal ion specificity and polymerisation of the protein. Additionally, both temperature-dependent CD analysis and temperature-dependent activity assays demonstrated that this domain greatly contributes to the thermo-tolerance of the host protein. We thus assumed that the NTD might provide an outer envelope that covers the temperature-sensitive hydrophobic residues or cavities on the surface of the active SODA "core" and improves the formation of hydrogen bonds or polar interactions between the monomers without affecting the interactions in the inner SODA "core", which contributes the metal binding site and is important for tetramer formation. Additionally, artificially fusing the NTD to the mesophilic SODA$_{BSn5}$, a close homolog of SODA$_{NG2215}$, led to a moderately thermophilic enzyme (OAT changed from 30 to 55°C). In contrast, SOD$_{NG2215}$ can tolerate higher temperatures, indicating that the NTD has evolved to be a well-matched heat-resistant partner to SODA$_{NG2215}$ over a long period.

In conclusion, to our knowledge, various factors determine protein thermostability. Some proteins even evolved more than one strategy to maintain their thermal tolerance. Herein, a new mechanism of protein thermostability defined by a unique peptide was discovered. The ability of the SOD$_{NG2215}$ NTD to improve the heat and stress resistance of host proteins could be highly useful in generating thermostable SODs for industrial applications. Work to determine the crystal structure of these enzymes is underway and could help to clearly reveal the mechanism of the improved thermostability conferred by the NTD to SODs.

1. Fridovich, I. Superoxide radical and superoxide dismutases. *Annu. Rev. Biochem.* **64**, 97–112 (1995).

2. Bannister, J. V., Bannister, W. H. & Rotilio, G. Aspects of the structure, function, and applications of superoxide dismutase. *CRC Crit. Rev. Biochem.* **22**, 111–180 (1987).

3. Bafana, A., Dutt, S., Kumar, S. & Ahuja, P. S. Superoxide dismutase: an industrial perspective. *Crit. Rev. Biotechnol.* **31**, 65–76 (2011).

4. Wuerges, J. *et al.* Crystal structure of nickel-containing superoxide dismutase reveals another type of active site. *Proc. Natl. Acad. Sci. USA* **101**, 8569–8574 (2004).

5. Miller, A. F. Superoxide dismutases: ancient enzymes and new insights. *FEBS Lett.* **586**, 585–595 (2012).

6. J Jackson, T. A. & Brunold, T. C. Combined spectroscopic/computational studies on Fe- and Mn-dependent superoxide dismutases: insights into second-sphere tuning of active site properties. *Acc. Chem. Res.* **37**, 461–470 (2004).

7. Angelova, M. *et al.* A novel glycosylated Cu/Zn-containing superoxide dismutase: production and potential therapeutic effect. *Microbiology* **147**, 1641–1650 (2001).

8. Cullen, J. J. *et al.* The role of manganese superoxide dismutase in the growth of pancreatic adenocarcinoma. *Cancer Res.* **63**, 1297–1303 (2003).

9. Emerit, J., Samuel, D. & Pavio, N. Cu-Zn super oxide dismutase as a potential antifibrotic drug for hepatitis C related fibrosis. *Biomed. Pharmacother.* **60**, 1–4 (2006).

10. Luisa, C. M. *et al.* Superoxide dismutase entrapped in long-circulating liposomes: formulation design and therapeutic activity in rat adjuvant arthritis. *Biochim. Biophys. Acta.* **1564**, 227–236 (2002).

11. Melov, S. *et al.* Extension of life-span with superoxide dismutase/catalase mimetics. *Science* **289** (2000).

12. Yunoki, M., Kawauchi, M., Ukita, N., Sugiura, T. & Ohmoto, T. Effects of lecithinized superoxide dismutase on neuronal cell loss in CA3 hippocampus after traumatic brain injury in rats. *Surg. Neurol.* **59**, 156–160; discussion 160–151 (2003).

13. Lim, J. H. *et al.* The crystal structure of an Fe-superoxide dismutase from the hyperthermophile *Aquifex pyrophilus* at 1.9 A resolution: structural basis for thermostability. *J. Mol. Biol.* **270**, 259–274 (1997).

14. Yamano, S. & Maruyama, T. An azide-insensitive superoxide dismutase from a hyperthermophilic archaeon, *Sulfolobus solfataricus*. *J. Biochem.* **125**, 186–193 (1999).

15. Yamano, S., Sako, Y., Nomura, N. & Maruyama, T. A cambialistic SOD in a strictly aerobic hyperthermophilic archaeon, *Aeropyrum pernix*. *J. Biochem.* **126**, 218–225 (1999).

16. Whittaker, M. M. & Whittaker, J. W. Recombinant superoxide dismutase from a hyperthermophilic archaeon, *Pyrobaculum aerophilium*. *J. Biol. Inorg. Chem.* **5**, 402–408 (2000).

17. Gligic, L., Radulovic, Z. & Zavisic, G. Superoxide dismutase biosynthesis by two thermophilic bacteria. *Enzyme Microb. Technol.* **27**, 789–792 (2000).

18. Lancaster, V. L., LoBrutto, R., Selvaraj, F. M. & Blankenship, R. E. A cambialistic superoxide dismutase in the thermophilic photosynthetic bacterium *Chloroflexus aurantiacus*. *J. Bacteriol.* **186**, 3408–3414 (2004).

19. Li, D. C., Gao, J., Li, Y. L. & Lu, J. A thermostable manganese-containing superoxide dismutase from the thermophilic fungus *Thermomyces lanuginosus*. *Extremophiles* **9**, 1–6 (2005).

20. Boyadzhieva, I. P., Atanasova, M. & Emanuilova, E. A novel, thermostable manganese-containing superoxide dismutase from *Bacillus licheniformis*. *Biotechnol. Lett.* **32**, 1893–1896 (2010).

21. Zhang, L. Q. *et al.* Expression of a novel thermostable Cu, Zn-superoxide dismutase from *Chaetomium thermophilum* in *Pichia pastoris* and its antioxidant properties. *Biotechnol. Lett.* **33**, 1127–1132 (2011).

22. Liu, J., Yin, M., Zhu, H., Lu, J. & Cui, Z. Purification and characterization of a hyperthermostable Mn-superoxide dismutase from *Thermus thermophilus* HB27. *Extremophiles* **15**, 221–226 (2011).

23. Song, C., Sheng, L. & Zhang, X. Preparation and characterization of a thermostable enzyme (Mn-SOD) immobilized on supermagnetic nanoparticles. *Appl. Microbiol. Biotechnol.* **96**, 123–132 (2012).

24. Kumar, A., Dutt, S., Bagler, G., Ahuja, P. S. & Kumar, S. Engineering a thermo-stable superoxide dismutase functional at sub-zero to >50 degrees C, which also tolerates autoclaving. *Sci. Rep.* **2**, 387 (2012).

25. Ding, Y., Cai, Y., Han, Y., Zhao, B. & Zhu, L. Application of principal component analysis to determine the key structural features contributing to iron superoxide dismutase thermostability. *Biopolymers* **97**, 864–872 (2012).

26. Wang, S. *et al.* Multistate folding of a hyperthermostable Fe-superoxide dismutase (TcSOD) in guanidinium hydrochloride: The importance of the quaternary structure. *Biochim. Biophys. Acta.* **1784**, 445–454 (2008).

27. Lim, J. H. *et al.* Mutational effects on thermostable superoxide dismutase from *Aquifex pyrophilus*: understanding the molecular basis of protein thermostability. *Biochem. Biophys. Res. Commun.* **288**, 263–268 (2001).

28. Dello, R. A., Rullo, R., Nitti, G., Masullo, M. & Bocchini, V. Iron superoxide dismutase from the archaeon *Sulfolobus solfataricus*: average hydrophobicity and amino acid weight are involved in the adaptation of proteins to extreme environments. *Biochim. Biophys. Acta.* **1343**, 23–30 (1997).

29. Knapp, S. *et al.* Refined crystal structure of a superoxide dismutase from the hyperthermophilic archaeon *Sulfolobus acidocaldarius* at 2.2 A resolution. *J. Mol. Biol.* **285**, 689–702 (1999).

30. Feng, L. *et al.* Genome and proteome of long-chain alkane degrading *Geobacillus thermodenitrificans* NG80-2 isolated from a deep-subsurface oil reservoir. *Proc. Natl. Acad. Sci. USA* **104**, 5602–5607 (2007).

31. Zou, Y. *et al.* Identification of three Superoxide dismutase genes from a *Geobacillus* sp. *Protein J.* **30**, 66–71 (2011).

32. Larkin, M. A. *et al.* Clustal W and Clustal X version 2.0. *Bioinformatics* **23**, 2947–2948 (2007).

33. Crooks, G. E., Hon, G., Chandonia, J. M. & Brenner, S. E. WebLogo: a sequence logo generator. *Genome Res.* **14**, 1188–1190 (2004).

34. Bradford, M. M. A rapid and sensitive method for the quantitation of microgram quantities of protein utilizing the principle of protein-dye binding. *Anal. Biochem.* **72**, 248–254 (1976).

35. Laemmli, U. K. Cleavage of structural proteins during the assembly of the head of bacteriophage T4. *Nature* **227**, 680–685 (1970).

36. Beauchamp, C. & Fridovich, I. Superoxide dismutase: improved assays and an assay applicable to acrylamide gels. *Anal. Biochem.* **44**, 276–287 (1971).

37. Nam, J. S., Yoon, J. H., Lee, H. I., Kim, S. W. & Ro, Y. T. Molecular cloning, purification, and characterization of a superoxide dismutase from a fast-growing *Mycobacterium* sp. Strain JC1 DSM 3803. *J. Microbiol.* **49**, 399–406 (2011).

38. Zhu, Y., Wang, G., Ni, H., Xiao, A. & Cai, H. Cloning and characterization of a new manganese superoxide dismutase from deep-sea thermophile *Geobacillus* sp. EPT3. *World J. Microbiol. Biotechnol.* **30**, 1347–1357 (2014).

39. Areekit, S. *et al.* Cloning, expression, and characterization of thermotolerant manganese superoxide dismutase from *Bacillus* sp. MHS47. *Int. J. Mol. Sci.* **12**, 844–856 (2011).

40. Song, N. N., Zheng, Y., E, S. J. & Li, D. C. Cloning, expression, and characterization of thermostable manganese superoxide dismutase from *Thermoascus aurantiacus* var. *levisporus*. *J. Microbiol.* **47**, 123–130 (2009).

41. Chen, Y. H., Yang, J. T. & Chau, K. H. Determination of the helix and beta form of proteins in aqueous solution by circular dichroism. *Biochemistry* **13**, 3350–3359 (1974).

42. Cooper, T. M. & Woody, R. W. The effect of conformation on the CD of interacting helices: a theoretical study of tropomyosin. *Biopolymers* **30**, 657–676 (1990).

43. Brown, J. E. & Klee, W. A. Helix-coil transition of the isolated amino terminus of ribonuclease. *Biochemistry* **10**, 470–476 (1971).

44. Nakamura, T. *et al.* Crystal structure of the cambialistic superoxide dismutase from *Aeropyrum pernix* K1--insights into the enzyme mechanism and stability. *FEBS J.* **278**, 598–609 (2011).

45. Nazina, T. N. *et al.* Taxonomic study of aerobic thermophilic bacilli: descriptions of *Geobacillus subterraneus* gen. nov., sp. nov. and *Geobacillus uzenensis* sp. nov. from petroleum reservoirs and transfer of *Bacillus stearothermophilus*, *Bacillus thermocatenulatus*, *Bacillus thermoleovorans*, *Bacillus kaustophilus*, *Bacillus thermoglucosidasius* and *Bacillus thermodenitrificans* to *Geobacillus* as the combinations *G. stearothermophilus*, *G. thermocatenulatus*, *G. thermoleovorans*, *G. kaustophilus*, *G. thermoglucosidasius* and *G. thermodenitrificans*. *Int. J. Syst. Evol. Microbiol.* **51**, 433–446 (2001).

46. Daniel, R. M., Danson, M. J., Eisenthal, R., Lee, C. K. & Peterson, M. E. New parameters controlling the effect of temperature on enzyme activity. *Biochem. Soc. Trans.* **35**, 1543–1546 (2007).

47. Daniel, R. M. & Danson, M. J. A new understanding of how temperature affects the catalytic activity of enzymes. *Trends Biochem. Sci.* **35**, 584–591 (2010).

48. Amo, T., Atomi, H. & Imanaka, T. Biochemical properties and regulated gene expression of the superoxide dismutase from the facultatively aerobic hyperthermophile *Pyrobaculum calidifontis*. *J. Bacteriol.* **185**, 6340–6347 (2003).

49. Vieille, C. & Zeikus, G. J. Hyperthermophilic enzymes: sources, uses, and molecular mechanisms for thermostability. *Microbiol. Mol. Biol. Rev.* **65**, 1–43 (2001).

50. Niehaus, F., Bertoldo, C., Kahler, M. & Antranikian, G. Extremophiles as a source of novel enzymes for industrial application. *Appl. Microbiol. Biotechnol.* **51**, 711–729 (1999).

51. Kumar, S., Tsai, C. J. & Nussinov, R. Factors enhancing protein thermostability. *Protein Eng.* **13**, 179–191 (2000).

52. Berezovsky, I. N., Tumanyan, V. G. & Esipova, N. G. Representation of amino acid sequences in terms of interaction energy in protein globules. *FEBS Lett.* **418**, 43–46 (1997).

53. Sadeghi, M., Naderi-Manesh, H., Zarrabi, M. & Ranjbar, B. Effective factors in thermostability of thermophilic proteins. *Biophys. Chem.* **119**, 256–270 (2006).

54. Schumann, J., Bohm, G., Schumacher, G., Rudolph, R. & Jaenicke, R. Stabilization of creatinase from *Pseudomonas putida* by random mutagenesis. *Protein Sci.* **2**, 1612–1620 (1993).

55. Berezovsky, I. N. & Shakhnovich, E. I. Physics and evolution of thermophilic adaptation. *Proc. Natl. Acad. Sci. USA* **102**, 12742–12747 (2005).

56. Hurley, J. H., Baase, W. A. & Matthews, B. W. Design and structural analysis of alternative hydrophobic core packing arrangements in bacteriophage T4 lysozyme. *J. Mol. Biol.* **224**, 1143–1159 (1992).

57. Jaenicke, R. & Bohm, G. The stability of proteins in extreme environments. *Curr. Opin. Struct. Biol.* **8**, 738–748 (1998).

58. Querol, E., Perez-Pons, J. A. & Mozo-Villarias, A. Analysis of protein conformational characteristics related to thermostability. *Protein Eng.* **9**, 265–271 (1996).

59. Vetriani, C. *et al.* Protein thermostability above 100 degreesC: a key role for ionic interactions. *Proc. Natl. Acad. Sci. USA* **95**, 12300–12305 (1998).

60. Thompson, M. J. & Eisenberg, D. Transproteomic evidence of a loop-deletion mechanism for enhancing protein thermostability. *J. Mol. Biol.* **290**, 595–604 (1999).

61. Rader, A. J., Yennamalli, R. M., Harter, A. K. & Sen, T. Z. A rigid network of long-range contacts increases thermostability in a mutant endoglucanase. *J. Biomol. Struct. Dyn.* **30**, 628–637 (2012).

62. Ding, M., Teng, Y., Yin, Q., Zhao, J. & Zhao, F. The N-terminal cellulose-binding domain of EGXA increases thermal stability of xylanase and changes its specific activities on different substrates. *Acta. Biochim. Biophys. Sin.* **40**, 949–954 (2008).

Acknowledgments

Author contributions

W.W. and T.M. contributed equally to this work. W.W. and J.C. designed all the research and analyzed the data. W.W., T.M. and J.C. performed the experiments and wrote the manuscript. B.Z., N.Y., M.L., L.C., G.L. and Z.M. carried out some experiments and analyzed some data. All authors reviewed and approved the manuscript.

Additional information